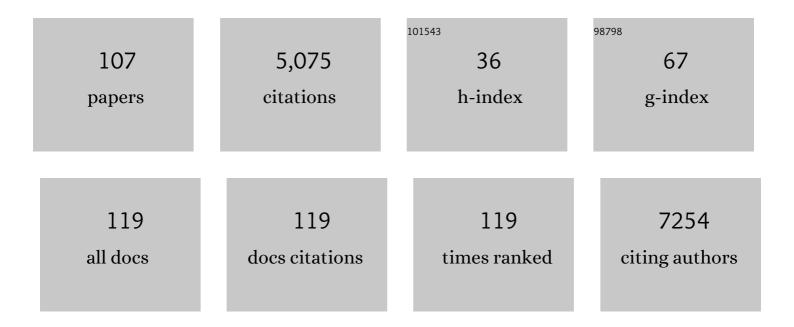
Takuya Hayashi

List of Publications by Year in descending order

Source: https://exaly.com/author-pdf/1263496/publications.pdf Version: 2024-02-01



#	Article	IF	CITATIONS
1	Human iPS cell-derived dopaminergic neurons function in a primate Parkinson's disease model. Nature, 2017, 548, 592-596.	27.8	528
2	Dopaminergic neurons generated from monkey embryonic stem cells function in a Parkinson primate model. Journal of Clinical Investigation, 2005, 115, 102-109.	8.2	418
3	Mechanisms underlying gait disturbance in Parkinson's disease. Brain, 1999, 122, 1271-1282.	7.6	266
4	Direct Comparison of Autologous and Allogeneic Transplantation of iPSC-Derived Neural Cells in the Brain of a Nonhuman Primate. Stem Cell Reports, 2013, 1, 283-292.	4.8	233
5	Dorsolateral prefrontal and orbitofrontal cortex interactions during self-control of cigarette craving. Proceedings of the National Academy of Sciences of the United States of America, 2013, 110, 4422-4427.	7.1	206
6	Circulating CD34-Positive Cells Provide an Index of Cerebrovascular Function. Circulation, 2004, 109, 2972-2975.	1.6	186
7	Transient Neural Activity in the Medial Superior Frontal Gyrus and Precuneus Time Locked with Attention Shift between Object Features. NeuroImage, 1999, 10, 193-199.	4.2	178
8	MHC matching improves engraftment of iPSC-derived neurons in non-human primates. Nature Communications, 2017, 8, 385.	12.8	178
9	Neurite imaging reveals microstructural variations in human cerebral cortical gray matter. NeuroImage, 2018, 182, 488-499.	4.2	164
10	Prolonged Maturation Culture Favors a Reduction in the Tumorigenicity and the Dopaminergic Function of Human ESCâ€Đerived Neural Cells in a Primate Model of Parkinson's Disease. Stem Cells, 2012, 30, 935-945.	3.2	155
11	Cerebral cortical folding, parcellation, and connectivity in humans, nonhuman primates, and mice. Proceedings of the National Academy of Sciences of the United States of America, 2019, 116, 26173-26180.	7.1	130
12	Survival of Human Induced Pluripotent Stem Cell–Derived Midbrain Dopaminergic Neurons in the Brain of a Primate Model of Parkinson's Disease. Journal of Parkinson's Disease, 2011, 1, 395-412.	2.8	110
13	Long-term observation of auto-cell transplantation in non-human primate reveals safety and efficiency of bone marrow stromal cell-derived Schwann cells in peripheral nerve regeneration. Experimental Neurology, 2010, 223, 537-547.	4.1	107
14	Accelerating the Evolution of Nonhuman Primate Neuroimaging. Neuron, 2020, 105, 600-603.	8.1	92
15	Endogenous dopamine release induced by repetitive transcranial magnetic stimulation over the primary motor cortex: an [11C]raclopride positron emission tomography study in anesthetized macaque monkeys. Biological Psychiatry, 2004, 55, 484-489.	1.3	91
16	Temporal Plasticity Involved in Recovery from Manual Dexterity Deficit after Motor Cortex Lesion in Macaque Monkeys. Journal of Neuroscience, 2015, 35, 84-95.	3.6	81
17	Rapid Quantitative Measurement of CMRO2 and CBF by Dual Administration of 15O-Labeled Oxygen and Water During a Single PET Scan—a Validation Study and Error Analysis in Anesthetized Monkeys. Journal of Cerebral Blood Flow and Metabolism, 2005, 25, 1209-1224.	4.3	76
18	An acute psychosocial stress enhances the neural response to smoking cues. Brain Research, 2009, 1293. 40-48.	2.2	74

#	Article	IF	CITATIONS
19	Motor recovery and microstructural change in rubro-spinal tract in subcortical stroke. NeuroImage: Clinical, 2014, 4, 201-208.	2.7	72
20	A Theoretical Model of Oxygen Delivery and Metabolism for Physiologic Interpretation of Quantitative Cerebral Blood Flow and Metabolic Rate of Oxygen. Journal of Cerebral Blood Flow and Metabolism, 2003, 23, 1314-1323.	4.3	67
21	Towards HCP-Style macaque connectomes: 24-Channel 3T multi-array coil, MRI sequences and preprocessing. Neurolmage, 2020, 215, 116800.	4.2	67
22	Establishment of In Vivo Brain Imaging Method in Conscious Mice. Journal of Nuclear Medicine, 2010, 51, 1068-1075.	5.0	66
23	Atrophy of the Corpus Callosum, Cortical Hypometabolism, and Cognitive Impairment in Corticobasal Degeneration. Archives of Neurology, 1998, 55, 609.	4.5	65
24	Gene Transfer of Hepatocyte Growth Factor Gene Improves Learning and Memory in the Chronic Stage of Cerebral Infarction. Hypertension, 2006, 47, 742-751.	2.7	65
25	Autologous mesenchymal stem cell–derived dopaminergic neurons function in parkinsonian macaques. Journal of Clinical Investigation, 2013, 123, 272-284.	8.2	63
26	Molecular, Functional, and Structural Imaging of Major Depressive Disorder. Neuroscience Bulletin, 2016, 32, 273-285.	2.9	62
27	Long-term effect of motor cortical repetitive transcranial magnetic stimulation induces. Annals of Neurology, 2004, 56, 77-85.	5.3	61
28	Neural activity during attention shifts between object features. NeuroReport, 1998, 9, 2633-2638.	1.2	58
29	The nonhuman primate neuroimaging and neuroanatomy project. NeuroImage, 2021, 229, 117726.	4.2	57
30	Diffusion Tensor Model links to Neurite Orientation Dispersion and Density Imaging at high b-value in Cerebral Cortical Gray Matter. Scientific Reports, 2019, 9, 12246.	3.3	49
31	Quantitative mapping of basal and vasareactive cerebral blood flow using split-dose 123I-iodoamphetamine and single photon emission computed tomography. NeuroImage, 2006, 33, 1126-1135.	4.2	45
32	Absolute quantitation of myocardial blood flow with 201Tl and dynamic SPECT in canine: optimisation and validation of kinetic modelling. European Journal of Nuclear Medicine and Molecular Imaging, 2008, 35, 896-905.	6.4	45
33	Parametric imaging of myocardial blood flow with 15O-water and PET using the basis function method. Journal of Nuclear Medicine, 2005, 46, 1219-24.	5.0	45
34	Rapid Quantitative <i>CBF</i> and <i>CMRO</i> ₂ Measurements from a Single <i>PET</i> Scan with Sequential Administration of Dual ¹⁵ O-Labeled Tracers. Journal of Cerebral Blood Flow and Metabolism, 2013, 33, 440-448.	4.3	41
35	An Alteration in the Lateral Geniculate Nucleus of Experimental Glaucoma Monkeys: In vivo Positron Emission Tomography Imaging of Glial Activation. PLoS ONE, 2012, 7, e30526.	2.5	40
36	Evaluation of a commercial PET tomograph-based system for the quantitative assessment of rCBF, rOEF and rCMRO2 by using sequential administration of 15O-labeled compounds. Annals of Nuclear Medicine, 2002, 16, 317-327.	2.2	37

#	Article	IF	CITATIONS
37	Brain/MINDS beyond human brain MRI project: A protocol for multi-level harmonization across brain disorders throughout the lifespan. NeuroImage: Clinical, 2021, 30, 102600.	2.7	34
38	Separation of input function for rapid measurement of quantitative CMRO2and CBF in a single PET scan with a dual tracer administration method. Physics in Medicine and Biology, 2007, 52, 1893-1908.	3.0	33
39	Use of a compact pixellated gamma camera for small animal pinhole SPECT imaging. Annals of Nuclear Medicine, 2006, 20, 409-416.	2.2	32
40	Delayed Postischemic Treatment With Fluvastatin Improved Cognitive Impairment After Stroke in Rats. Stroke, 2007, 38, 3251-3258.	2.0	32
41	Effects of patient movement on measurements of myocardial blood flow and viability in resting 15O-water PET studies. Journal of Nuclear Cardiology, 2012, 19, 524-533.	2.1	29
42	A new reconstruction strategy for image improvement in pinhole SPECT. European Journal of Nuclear Medicine and Molecular Imaging, 2004, 31, 1166-72.	6.4	27
43	Scan–rescan and inter-vendor reproducibility of neurite orientation dispersion and density imaging metrics. Neuroradiology, 2020, 62, 483-494.	2.2	26
44	Neuronal nitric oxide has a role as a perfusion regulator and a synaptic modulator in cerebellum but not in neocortex during somatosensory stimulation—An animal PET study. Neuroscience Research, 2002, 44, 155-165.	1.9	25
45	Comparison of Striatal Dopamine D2 Receptors in Parkinson's Disease and Progressive Supranuclear Palsy Patients Using [¹²³ I] Iodobenzofuran Singleâ€Photon Emission Computed Tomography. Journal of Neuroimaging, 2002, 12, 316-324.	2.0	25
46	Objective and quantitative evaluation of motor function in a monkey model of Parkinson's disease. Journal of Neuroscience Methods, 2010, 190, 198-204.	2.5	25
47	Application of a cell microarray chip system for accurate, highly sensitive and rapid diagnosis for malaria in Uganda. Scientific Reports, 2016, 6, 30136.	3.3	24
48	A Physiologic Model for Recirculation Water Correction in CMRO ₂ Assessment with ¹⁵ O ₂ Inhalation PET. Journal of Cerebral Blood Flow and Metabolism, 2009, 29, 355-364.	4.3	23
49	Comparative connectomics of the primate social brain. NeuroImage, 2021, 245, 118693.	4.2	23
50	Minimal specifications for non-human primate MRI: Challenges in standardizing and harmonizing data collection. NeuroImage, 2021, 236, 118082.	4.2	22
51	Toward next-generation primate neuroscience: A collaboration-based strategic plan for integrative neuroimaging. Neuron, 2022, 110, 16-20.	8.1	22
52	Empirical transmit field bias correction of T1w/T2w myelin maps. NeuroImage, 2022, 258, 119360.	4.2	20
53	Linkage Between the Midline Cortical Serotonergic System and Social Behavior Traits: Positron Emission Tomography Studies of Common Marmosets. Cerebral Cortex, 2013, 23, 2136-2145.	2.9	19
54	Premotor Cortical-Cerebellar Reorganization in a Macaque Model of Primary Motor Cortical Lesion and Recovery. Journal of Neuroscience, 2019, 39, 8484-8496.	3.6	19

#	Article	IF	CITATIONS
55	Low Immunogenicity and Immunosuppressive Properties of Human ESC- and iPSC-Derived Retinas. Stem Cell Reports, 2021, 16, 851-867.	4.8	19
56	Cerebral glucose metabolism in unilateral entorhinal cortex-lesioned rats. NeuroReport, 1999, 10, 2113-2118.	1.2	18
57	lssues in measuring glucose metabolism of rat brain using PET: the effect of Harderian glands on the frontal lobe. Neuroscience Letters, 1998, 255, 99-102.	2.1	17
58	Quantitative evaluation of changes in binding potential with a simplified reference tissue model and multiple injections of [11C]raclopride. NeuroImage, 2009, 47, 1639-1648.	4.2	17
59	Glucose metabolism in the rat frontal cortex recovered without the recovery of choline acetyltransferase activity after lesioning of the nucleus basalis magnocellularis. Neuroscience Letters, 2000, 280, 9-12.	2.1	14
60	Sensory stimulation accelerates dopamine release in the basal ganglia. Brain Research, 2004, 1026, 179-184.	2.2	13
61	Selective Cerebral Hematocrit Decrease in the Centrum Semiovale after Carotid Artery Occlusion: A PET Study. Journal of Cerebral Blood Flow and Metabolism, 1999, 19, 109-114.	4.3	12
62	Use of a clinical MRI scanner for preclinical research on rats. Radiological Physics and Technology, 2009, 2, 13-21.	1.9	11
63	Development of motion correction technique for cardiac 15O-water PET study using an optical motion tracking system. Annals of Nuclear Medicine, 2010, 24, 1-11.	2.2	11
64	Association between affective temperaments and regional gray matter volume in healthy subjects. Journal of Affective Disorders, 2014, 155, 169-173.	4.1	11
65	Understanding of cerebral energy metabolism by dynamic living brain slice imaging system with [18F]FDG. Neuroscience Research, 2005, 52, 357-361.	1.9	10
66	Sensitivity of kinetic macro parameters to changes in dopamine synthesis, storage, and metabolism: A simulation study for [¹⁸ F]FDOPA PET by a model with detailed dopamine pathway. Synapse, 2011, 65, 751-762.	1.2	10
67	Quantification of regional cerebral blood flow in rats using an arteriovenous shunt and micro-PET. Nuclear Medicine and Biology, 2012, 39, 730-741.	0.6	10
68	Kinetics of neurodegeneration based on a risk-related biomarker in animal model of glaucoma. Molecular Neurodegeneration, 2013, 8, 4.	10.8	10
69	Visualization of drug translocation in the nasal cavity and pharmacokinetic analysis on nasal drug absorption using positron emission tomography in the rat. European Journal of Pharmaceutics and Biopharmaceutics, 2016, 99, 45-53.	4.3	10
70	Anatomical variability, multi-modal coordinate systems, and precision targeting in the marmoset brain. NeuroImage, 2022, 250, 118965.	4.2	10
71	The effect of sequential lesioning in the basal forebrain on cerebral cortical glucose metabolism in rats. An animal positron emission tomography study. Brain Research, 1999, 837, 75-82.	2.2	9
72	Enhanced carbonyl stress and disrupted white matter integrity in schizophrenia. Schizophrenia Research, 2020, 223, 242-248.	2.0	9

#	Article	IF	CITATIONS
73	Measurement of Density and Affinity for Dopamine D2 Receptors by a Single Positron Emission Tomography Scan with Multiple Injections of [11C]raclopride. Journal of Cerebral Blood Flow and Metabolism, 2010, 30, 663-673.	4.3	8
74	Development of a highly sensitive, quantitative, and rapid detection system for Plasmodium falciparum-infected red blood cells using a fluorescent blue-ray optical system. Biosensors and Bioelectronics, 2019, 132, 375-381.	10.1	8
75	Quantification of regional myocardial oxygen metabolism in normal pigs using positron emission tomography with injectable 150-02. European Journal of Nuclear Medicine and Molecular Imaging, 2010, 37, 377-385.	6.4	7
76	Quantitative assessment of regional cerebral blood flow by dynamic susceptibility contrast-enhanced MRI, without the need for arterial blood signals. Physics in Medicine and Biology, 2012, 57, 7873-7892.	3.0	7
77	Development of a quantitative, portable, and automated fluorescent blue-ray device-based malaria diagnostic equipment with an on-disc SiO2 nanofiber filter. Scientific Reports, 2020, 10, 6585.	3.3	7
78	Chapter 8 A coil for magnetic stimulation of the macaque monkey brain. Supplements To Clinical Neurophysiology, 2003, 56, 75-80.	2.1	6
79	Influence of residual oxygen-15-labeled carbon monoxide radioactivity on cerebral blood flow and oxygen extraction fraction in a dual-tracer autoradiographic method. Annals of Nuclear Medicine, 2009, 23, 363-371.	2.2	5
80	Three-dimensional quantitation of regional cerebral blood flow in mice using a high-resolution pinhole SPECT system and 1231-iodoamphetamine. Nuclear Medicine and Biology, 2011, 38, 1157-1164.	0.6	5
81	A novel Tungsten-based fiducial marker for multi-modal brain imaging. Journal of Neuroscience Methods, 2019, 323, 22-31.	2.5	5
82	The posterior parietal cortex contributes to visuomotor processing for saccades in blindsight macaques. Communications Biology, 2021, 4, 278.	4.4	5
83	Personality, subjective well-being, and the serotonin 1a receptor gene in common marmosets (Callithrix jacchus). PLoS ONE, 2021, 16, e0238663.	2.5	5
84	Optimization of transmission scan duration for 150 PET study with sequential dual tracer administration using N-index. Annals of Nuclear Medicine, 2010, 24, 413-420.	2.2	4
85	Quantification in SPECT cardiac imaging. Journal of Nuclear Medicine, 2003, 44, 40-2.	5.0	4
86	Neuroimaging for optimization of stem cell therapy in Parkinson's disease. Expert Opinion on Biological Therapy, 2013, 13, 1631-1638.	3.1	3
87	Quantification of receptor activation by oxytocin and vasopressin in endocytosis-coupled bioluminescence reduction assay using nanoKAZ. Analytical Biochemistry, 2018, 549, 174-183.	2.4	3
88	Affective temperaments are associated with the white matter microstructure in healthy participants. Bipolar Disorders, 2019, 21, 539-546.	1.9	3
89	Development of injectable O-15 oxygen and its application for estimation of OEF. International Congress Series, 2004, 1265, 262-265.	0.2	2
90	A physiological model for cerebral oxygen delivery and consumption and effective oxygen diffusibility evaluated by PET. International Congress Series, 2004, 1265, 228-237.	0.2	2

#	Article	IF	CITATIONS
91	Measurement of cerebral blood flow with dynamic susceptibility contrast MRI and comparison with O-15 positron emission tomography. International Congress Series, 2004, 1265, 150-158.	0.2	2
92	Chapter 24 Repetitive transcranial magnetic stimulation (rTMS) in monkeys. Supplements To Clinical Neurophysiology, 2006, 59, 173-181.	2.1	2
93	The role of neuronal nitric oxide in the regional neurovascular coupling. International Congress Series, 2002, 1235, 197-204.	0.2	1
94	Improved parametric images of blood flow and vascular volume by. International Congress Series, 2004, 1265, 79-83.	0.2	1
95	Evaluation of utility of asymmetric index for count-based oxygen extraction fraction on dual-tracer autoradiographic method for chronic unilateral brain infarction. Annals of Nuclear Medicine, 2009, 23, 533-539.	2.2	1
96	Rapid CBF/CMRO2 measurement in a single PET scan with dual tracer administration. Journal of Cerebral Blood Flow and Metabolism, 2005, 25, S672-S672.	4.3	1
97	Model-based background compensation for repeat PET study with multiple tracer administration. IFAC Postprint Volumes IPPV / International Federation of Automatic Control, 2003, 36, 29-34.	0.4	0
98	Therapeutic mechanism of repetitive transcranial magnetic stimulation (rTMS)—a monkey PET study. International Congress Series, 2004, 1264, 186-190.	0.2	0
99	Future perspectives in in vivo quantitation of bio-physiological parameters. International Congress Series, 2004, 1264, 148-157.	0.2	0
100	Adenosine-induced myocardial flow reactivity in pig as assessed with O-15 water PET. International Congress Series, 2004, 1264, 117-125.	0.2	0
101	Dynamic spectroscopy of hyperpolarized Xe-129 in rat lung. International Congress Series, 2004, 1265, 131-138.	0.2	0
102	Image improvement in pinhole SPECT using complete data acquisition combined with statistical image reconstruction. International Congress Series, 2004, 1265, 101-105.	0.2	0
103	A role of dorsolateral prefrontal cortex in cue-induced craving. Neuroscience Research, 2007, 58, S66.	1.9	0
104	Sensitivity of FDOPA kinetic macro-parameters to changes in Parkinson's disease: Evaluation for noise influence in [18F]FDOPA PET data. NeuroImage, 2010, 52, S171.	4.2	0
105	Development of a Hyperpolarized 129Xe System on 3T for the Rat Lungs. Magnetic Resonance in Medical Sciences, 2004, 3, 1-9.	2.0	0
106	Development of sinogram-based estimation method of delay time of arterial input function with O-15 tracer and PET study. Journal of Cerebral Blood Flow and Metabolism, 2005, 25, S674-S674.	4.3	0
107	A spatially embedded cortical connectome reveals complex transformations. Neuron, 2022, 110, 185-187.	8.1	0